



## RESEARCH ARTICLE

### NUMERICAL STUDY OF MAGNETO THERMAL AIR CONVECTION IN A RECTANGULAR ENCLOSURE

\*Siriman SQUARE, Omar Ngor THIAM, Oumar DRAME, Abou NDIAYE Joseph SARR and Momodou Lamine SOW

Fluid Mechanics and Applications Laboratory, Physics Department, Sciences and technologies Faculty, Cheikh Anta DIOP University, Dakar-Fann, Senegal

#### ARTICLE INFO

##### Article History:

Received 20<sup>th</sup> September, 2020  
Received in revised form  
16<sup>th</sup> October, 2020  
Accepted 24<sup>th</sup> November, 2020  
Published online 30<sup>th</sup> December, 2020

##### Keywords:

Magneto Thermal Convection, Finite Volumes, SIMPLER Algorithm, Ansys Fluent.

#### ABSTRACT

In this paper we have done the numerical study of the magneto thermal convection of air in a rectangular enclosure. We use the finite volume method to solve numerically the dimensionless Navier-Stokes equations that govern our flow. This resolution goes through the sequences of the SIMPLER algorithm which summarizes the different calculation steps. An essential part of the literature in the field is in agreement with the results of our numerical simulation. Indeed, it is shown that the longer the calculation time, the more the effects were visible on the velocity profile as well as those of the isotherms in the fluid domain. Similarly, the parallel orientation of the magnetic field with respect to the flow favored an increase in the velocity in the direction of flow due to the presence of the magnetic force. The representation of variations in the Nusselt number shows that it varies in opposite directions with the increase in temperature near heated walls.

#### INTRODUCTION

To find a solution to a physical problem one passes inevitably by one of the three methods. The first consists in developing an experimental protocol with well-developed equipment, the second with an analytical or mathematical resolution, and the third is based on a numerical resolution procedure with initial conditions and well defined limits. As the equations of a magneto thermal convection phenomenon are complex and analytically insoluble, we use the finite volume method to solve them numerically. Several authors of the literature have attempted in the past to find solutions by various methods. This is how FaridBerahil and SmailBenissad(1) sought, using the finite volume method, to see the effects of volumetric heating on the structure of their flow in order to compare the best orientation of the magnetic field. The phenomenon of magneto thermal convection induced by the Kelvin force is explained by Masato Akamatsu et al. (2). They were able to explain the effects of this force on the velocity and temperature field in the absence of a gravitational field. Thus the number of Nusselt varies in the opposite direction with the increase of the magnetic field near the heated wall. In addition, Mouhamed A. Teamah et al. (3) Have made a numerical study of a double diffusion in a rectangular enclosure inclined with respect to the horizontal. They flowed in the presence of a constant magnetic field applied to the side walls. In another approach Xiao-Yan et al. (4) analyzed the detection of oxygen concentration using thermal magnetic convection. Their study is based on a numerical analysis which demonstrates that said convection promotes flow. Furthermore, Seyou Maki (5) studied the magnetothermal convection of water which depends on a magnetic susceptibility gradient. Where he shows that the importance of the latter depends not only on the magnetic conditions but also on the thermal properties of the fluid. Sebastien R. de Vaux (6) has also studied thermal convection in the presence of a magnetic field. It used volumetric heating by electromagnetic induction of fluids which makes it possible to simulate in the laboratory the volume power of nuclear decay by avoiding the use of radioactive materials. In the course of this paper, we will have to deal with two main parts. The mathematical and numerical model part, which is based on the dimensionless Navier-stokes equations closed by initial and boundary conditions and a numerical analysis based on the finite volume method with the resolution algorithm (SIMPLER) which explains the calculation steps well. Particular attention will be paid to the interpretation of the results from the numerical simulation. A conclusion and lines of research as well as a bibliographical review will close this paper.

#### MATERIALS AND METHODS

**Mathematical model:** The search for a solution to a physical problem passes by the development of mathematical equations in a system of coordinated suitable. The equations of Navier-stokes hereafter enables us to determine the behavior of the paramagnetic fluid well. In order to simplify and adapt the study to the behavior of our fluid, a certain number of hypotheses are put forward.

\*Corresponding author: Siriman SQUARE,

Fluid Mechanics and Applications Laboratory, Physics Department, Sciences and technologies Faculty, Cheikh Anta DIOP University, Dakar-Fann, Senegal.

**These assumptions are as follows:**

- The characteristic velocity of the flow is very low compared to the velocity of the adiabatic sound. It is therefore legitimate to neglect the powers of the forces of pressure and the forces of viscosity dissipated in heat before the other contributions.
- We assume that the magnetic field is variable and we neglect its side effects.
- We assume the energy variation due to negligible compressibility.
- We assume that the fluid flow is two-dimensional, laminar and unsteady.
- We assume negligible the work induced by the viscosity forces.

Taking into account these assumptions and the characteristic quantities. It comes the dimensionless equations below.

**Continuity**

$$\partial_y v' + \partial_z w' = 0 \quad (1.1)$$

**Momentum equation**

**y direction**

$$\partial_t v' + \partial_y \left[ v'v' - \frac{2}{R_e} \partial_y v' \right] + \partial_z \left[ v'w' - \frac{2}{R_e} \partial_z v' \right] = -\partial_y P' + Ne \cdot B' \partial_y B' \quad (1.2)$$

**z direction**

$$\partial_t w' + \partial_y \left[ v'w' - \frac{2}{R_e} \partial_y w' \right] + \partial_z \left[ w'w' - \frac{2}{R_e} \partial_z w' \right] = -\partial_z P' + Ne \cdot B' \partial_z B' \quad (1.3)$$

**Energy equation**

$$\partial_t T' + \partial_y \left[ v'T' - \frac{2}{R_e P_r} \partial_y T' \right] + \partial_z \left[ w'T' - \frac{2}{R_e P_r} \partial_z T' \right] = 0 \quad (1.4)$$

Where:  $Ne = \frac{t B_0^2}{\rho_0 U_0^2}$

With:

Let  $y' = \frac{y}{h}, z' = \frac{z}{h}$  be the dimensionless lengths in the y and z directions respectively.

Let  $T' = \frac{T - T_0}{\Delta T}$  be the dimensionless temperature.

Idem for  $v' = \frac{v}{u_0}, w' = \frac{w}{u_0}$  which represent the dimensionless velocities.

Let  $t' = \frac{t}{h / u_0}$  be the dimensionless time.

And  $\dots u_0^2$  which represents the dimensionless pressure of the fluid.

Finally  $\frac{g}{L}$  which represents the dimensionless magnitude of the acceleration of gravity.

$D_h = 2h$ , represents the hydraulic diameter as a function of the characteristic length of the flow.

BOUNDARY	DYNAMIQUES CONDITIONS	THERMALS CONDITIONS	MAGNETS CONDITIONS
At the Inlet $i = 1$	$w_{(1,j)} = U_0$	$T_{(1,j)} = T_e$ $p_{(1,j)} = p_e$	$B_{(1,j)} = 0$
Top and Bottom $j=1$ or $jm$ Et $1 \leq i \leq im/3$ for magnet field	$\frac{v_{(i,jm)} - v_{(i,jm-1)}}{2dy} = 0$ $w(i, 1 \text{ ou } jm) = 0; v(i, 1 \text{ ou } jm)$	$T_{(i,jm)} = T_p$ $\frac{p_{(i,jm)} - p_{(i,jm-1)}}{2dy} = 0$	$B_{(i,1 \text{ ou } jm)} = B_0(\sin\theta + \cos\theta)$
At the Outlet $i = im$	$\frac{v_{(im,j)} - v_{(im-1,j)}}{2dz} = 0$ $\frac{w_{(im,j)} - w_{(im-1,j)}}{2dz} = 0$	$\frac{T_{(im,j)} - T_{(im-1,j)}}{2dz} = 0$ $\frac{P_{(im,j)} - P_{(im-1,j)}}{2dz} = 0$	$B_{(im,j)} = 0$

**Numerical model:** The solution of these mathematical equations requires the use of a numerical method. The finite volume method is chosen to search for this solution. A brief summary of the finite volume method, followed by a presentation of the centered difference scheme and the sequence of the SIMPLER algorithm which summarizes the different stages of numerical calculation, is made.

The flow is laminar, unsteady and two-dimensional so the general transport equation takes the following form:

$$\frac{\partial}{\partial t}(\dots W) + \frac{\partial}{\partial x}(\dots uW) + \frac{\partial}{\partial y}(\dots vW) + \frac{\partial}{\partial z}(\dots wW) = \frac{\partial}{\partial x}\left(\Gamma \frac{\partial W}{\partial x}\right) + \frac{\partial}{\partial y}\left(\Gamma \frac{\partial W}{\partial y}\right) + \frac{\partial}{\partial z}\left(\Gamma \frac{\partial W}{\partial z}\right) + S_w \tag{1.5}$$

Where W represent the quantity transported,  $\Gamma$  the diffusion coefficient and  $S_w$  the source term.

The table below summarizes the system dependent variables.

	$\phi$	$\Gamma$	$S_\phi$
Mass conservation	1	0	0
Next (oy)	$v'$	$\frac{2}{Re}$	$\partial_y P' + Ne F_{my}$
Next (oz)	$w'$	$\frac{2}{Re}$	$\partial_z P' + Ne F_{mz}$
Thermal conservation	$T'$	1	0

Table 2. Summary of system dependent variables

Equation (1.5) above is a partial differential equation, after having discretized it will be possible to seek the successive values of. We use the conservative form to rewrite equation (2):

$$\partial_t (J_t) + \partial_z (J_z) + \partial_y (J_y) = S_w \tag{1.6}$$

with:

$$J_z = \dots W - \Gamma \frac{\partial W}{\partial z}$$

$$J_y = \dots W - \Gamma \frac{\partial W}{\partial y}$$

$$J_t = \dots W$$

$J_x$  and  $J_y$  represent the total flows across surfaces in the x and y directions.

Let's transform the writing of this differential transport equation into an algebraic equation system.

Let's integrate equation (1.6) on the control volume, it comes:

$$\int_{t+\Delta t}^{t+\Delta t + \Delta t} \int_{e}^{n} \int_{e}^{e} \left[ \partial_t (J_t) + \partial_x (J_x) + \partial_y (J_y) \right] dx dy dt = \int_{t+\Delta t}^{t+\Delta t + \Delta t} \int_{e}^{e} \int_{e}^{e} S_\phi dx dy dt \tag{1.7}$$

With:

A, which represents the total flow through the control volume.

B, which represents the source term.

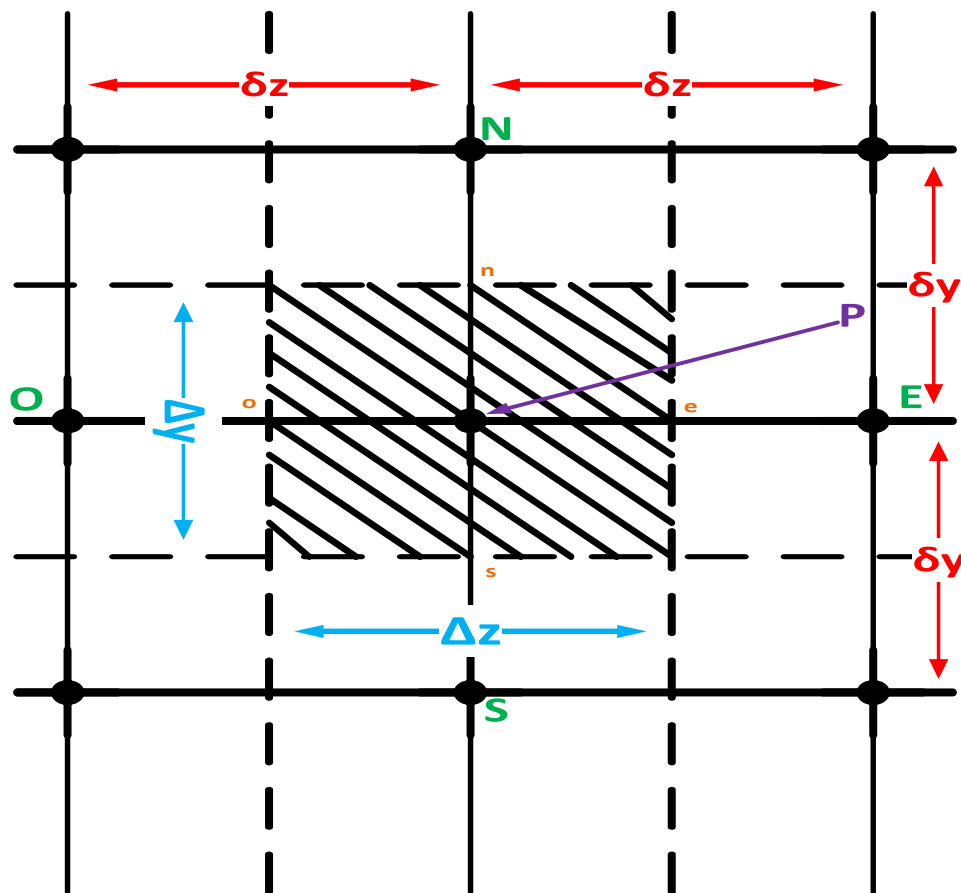


Figure 1. Two-dimensional view of the control volume

Let's take a number of hypotheses in order to approximate equation (1.7) in algebraic form. These assumptions are as follows:

- The variable varies linearly in the domain and this in the directions of y and z.
- The convective term is uniform across the walls.
- In the control volume, the source term is uniform.

**Integration of the total flow**

Let A be the total flow, integrate it on the control volume:

$$\begin{aligned}
 A &= \int_s^n \int_o^e \left[ \partial_x (J_x) + \partial_y (J_y) \right] dx dy \\
 A &= \left[ (J_y)_n - (J_y)_s \right] \int_o^e dx + \left[ (J_x)_e - (J_x)_o \right] \int_s^n dy \\
 A &= (J_y)_n \Delta x - (J_y)_s \Delta x + (J_x)_e \Delta y - (J_x)_o \Delta y
 \end{aligned}
 \tag{1.8}$$

Let's ask:

$$\begin{aligned}
 j_h &= (J_x)_h \Delta y \Delta z \\
 j_b &= (J_x)_b \Delta y \Delta z \\
 j_n &= (J_y)_n \Delta x \Delta z \\
 j_s &= (J_y)_s \Delta x \Delta z \\
 j_e &= (J_z)_e \Delta x \Delta y \\
 j_o &= (J_z)_o \Delta x \Delta y
 \end{aligned}
 \tag{1.9}$$

The expression of A becomes:

$$A = j_e - j_o + j_n - j_s
 \tag{1.10}$$

Integration of the source term

Let B be the term sources, let's integrate it into the control volume it comes:

$$\begin{aligned}
 B &= \int_s^n \int_o^e S_w dy dz = \left[ \int_o^e S_w dz \right] \int_s^n dy \\
 B &= \overline{S_w} \Delta y \Delta z
 \end{aligned}
 \tag{1.11}$$

With which represents the mean of the source term on the control volume, in the case where this mean depends on the system variables. This dependence is expressed by a linear relation, which will allow us to use the methods of resolution of the linear systems. Thus the source term is linearized to facilitate convergence. This linearization takes the following form:

$$\overline{S_w} = S_c + S_p W_p
 \tag{1.12}$$

Where is the constant part which does not depend explicitly on  $S_p$ ,  $S_p$  represents the slope. It is necessary that the coefficient  $S_p$  is lower than zero this so that the solution is numerically stable and that convergence is faster. Taking into account the relations (1.10) and (1.11) the equation (1.7) takes the form:

$$(j_n - j_s) + (j_e - j_o) = (S_c + W_p S_p) \Delta y \Delta z
 \tag{1.13}$$

Where  $j_i$  ( $i = e, o, n, s, h, b$ ) are the total flows evaluated on each side of the control volume. These flows are composed of two parts which are the convective flow and the diffusive one.

**Centered Difference scheme:** The variation of the variable between two adjacent nodes (7) must be expressed by a linear profile in order to evaluate the convective flow at the interface. However, the faces (e, o, n, s) being in the middle of the nodes (E, O, N, S) respectively, therefore the convective terms of the generalized variables can be presented by an interpolation according to the method below:

$$\left. \begin{aligned} W_e &= \frac{1}{2}(W_E + W_P) \\ W_o &= \frac{1}{2}(W_O + W_P) \\ W_n &= \frac{1}{2}(W_N + W_P) \\ W_s &= \frac{1}{2}(W_S + W_P) \end{aligned} \right\} \tag{1.14}$$

The diffusive parts are evaluated by approximating the derivatives by the differences which gives:

$$\left. \begin{aligned} \Gamma_e \left( \frac{\partial W}{\partial z} \right)_e &= \Gamma_e \frac{(W_E - W_P)}{(u z)_e} \\ \Gamma_o \left( \frac{\partial W}{\partial z} \right)_o &= \Gamma_o \frac{(W_P - W_O)}{(u z)_o} \\ \Gamma_n \left( \frac{\partial W}{\partial y} \right)_n &= \Gamma_n \frac{(W_N - W_P)}{(u z)_n} \\ \Gamma_s \left( \frac{\partial W}{\partial y} \right)_s &= \Gamma_s \frac{(W_P - W_S)}{(u z)_s} \end{aligned} \right\} \tag{1.15}$$

$$\left. \begin{aligned} \Gamma_e \left( \frac{\partial W}{\partial z} \right)_e &= \Gamma_e \frac{(W_E - W_P)}{(u z)_e} \\ \Gamma_o \left( \frac{\partial W}{\partial z} \right)_o &= \Gamma_o \frac{(W_P - W_O)}{(u z)_o} \\ \Gamma_n \left( \frac{\partial W}{\partial y} \right)_n &= \Gamma_n \frac{(W_N - W_P)}{(u z)_n} \\ \Gamma_s \left( \frac{\partial W}{\partial y} \right)_s &= \Gamma_s \frac{(W_P - W_S)}{(u z)_s} \end{aligned} \right\} \tag{1.16}$$

As we had in (1.13):  $(j_e - j_o) + (j_n - j_s) = (S_c + w_p S_p) \Delta y \Delta z$

And that:

$$\left\{ \begin{aligned} j_e &= \left[ \dots wW - \Gamma_e \left( \frac{\partial W}{\partial z} \right)_e \right] ; j_o = \left[ \dots wW - \Gamma_o \left( \frac{\partial W}{\partial z} \right)_o \right] \\ j_n &= \left[ \dots wW - \Gamma_n \left( \frac{\partial W}{\partial y} \right)_n \right] ; j_s = \left[ \dots wW - \Gamma_s \left( \frac{\partial W}{\partial y} \right)_s \right] \end{aligned} \right\} \tag{1.17}$$

$$j_e = \left[ \dots wW - \Gamma_e \left( \frac{\partial W}{\partial z} \right) \right]_e ; j_o = \left[ \dots wW - \Gamma_o \left( \frac{\partial W}{\partial z} \right) \right]_o$$

$$j_n = \left[ \dots wW - \Gamma_n \left( \frac{\partial W}{\partial y} \right) \right]_n ; j_s = \left[ \dots wW - \Gamma_s \left( \frac{\partial W}{\partial y} \right) \right]_s$$
(1.18)

With:

$$D_i = \frac{\Gamma_i}{(u y)_i} ; F_i = \dots U_i ; b = S_c \Delta y \Delta z$$

$$a_E = D_e - \frac{1}{2} F_e ; a_O = D_o + \frac{1}{2} F_o$$

$$a_N = D_n - \frac{1}{2} F_n ; a_S = D_s + \frac{1}{2} F_s$$
(1.19)

Or:

$$P_{e_i} = \frac{F_i}{D_i} = \frac{(u y)_i (\dots U_i)}{\Gamma_i}$$

$$a_E = D_e \left( 1 - \frac{1}{2} P_{e_e} \right) ; a_o = D_o \left( 1 + \frac{1}{2} P_{e_o} \right)$$

$$a_N = D_n \left( 1 - \frac{1}{2} P_{e_n} \right) ; a_S = D_s \left( 1 + \frac{1}{2} P_{e_s} \right)$$
(1.20)

Taking into account the second rule of the finite volume method which states that the coefficients  $a_i$  must always be positive. So after rearrangement we can write equation (1.13) in its discretized form as follows:

$$a_p W_p = a_E W_E + a_O W_O + a_N W_N + a_S W_S + b$$
(1.21)

With:

$$a_p = a_E + a_O + a_N + a_S - S_p \Delta y \Delta z$$
(1.22)

### SIMPLER ALGORITHM SEQUENCE

We can see below the sequence of the SIMPLER algorithm:

- 1 / Choose an initial guess velocity field.
- 2 / Calculate the coefficients of the momentum equations and deduce the pseudo-velocities
- 3 / Evaluate the source term b and solve the pressure equation.
- 4 / Use the pressure field to solve the momentum equations to obtain the velocities fields u and v.
- 5 / Calculate the source term b and solve the pressure correction equation.
- 6 / Correct the velocity field (do not correct the pressure).
- 7 / Solve the other transport equations of other scalars of the problem, such as temperature or concentration etc...
- 8 / Return to step 2. Repeat the calculations until all the variables converge.

Note here that the SIMPLER algorithm does not require an initial pressure field. The pressure is directly generated from the initialization of the velocity. Consequently, more consistent under relaxation coefficients can be used for the velocities. Best of all, no under relaxation is needed for the pressure. It is true that an iteration following the SIMPLER algorithm requires approximately more time than that of SIMPLE, but this effort is largely compensated by the consistent reduction in number of iterations necessary for convergence. (9)

### RESULTS

**Mesh sensibility:** On the table below, we notice for the densest mesh 71×71 the maximum value of the axial temperature of the flow is weak compared to the two other less dense meshes 71×51 and 71×15 with a relative error of the order of 0.0004% between the maximum values evaluated. In addition, a less dense mesh 71×15 allows us to have the highest axial temperature, which motivates the choice of this mesh compared to the other two in the rest of the study.

Mesh density	71*71	71*51	71*15
Maximum temperature	0.4958	0.4960	0.4962

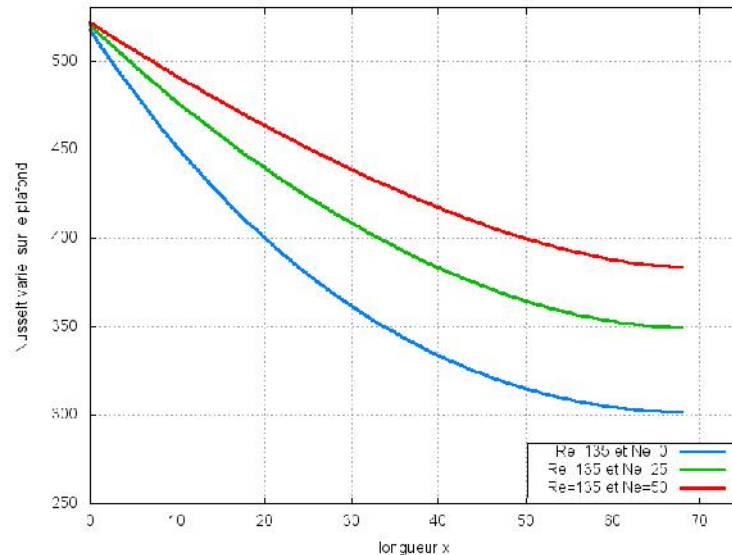


Figure 2. Mesh sensibility

**Validation:** In order to validate the results of our simulations, we compare them to those of the ANSYS fluent software (benchmark) (8). The entry and exit conditions are the same as the conditions on the walls in the absence of magnetic field. On the figure on the left below, we have the results of the simulation of the thermal convection of the air with as number of cells equal to 1065 in an irregular mesh  $71 \times 15$  for and a time step  $\Delta t = 1.10^{-2}$ . The same conditions are repeated for the simulation with the FORTRAN language, except that here we use dimensionless numbers like the Reynolds number which takes the value  $Re = 200$ . By analyzing the typology of the contours we notice that the results are similar to some differences for a laminar flow regime.

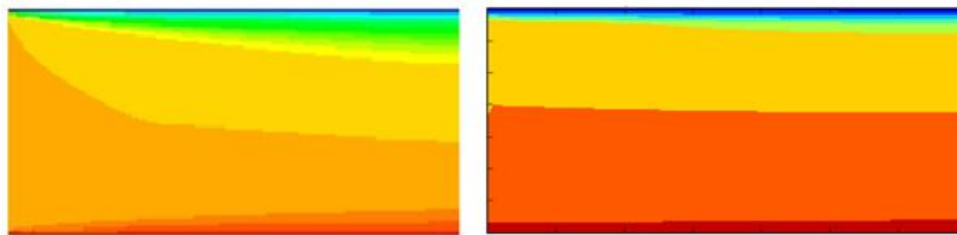


Figure 3. Temperature contour observed for ANSYS FLUENT and for us at  $Re = 200$

**DISCUSSIONS**

**Influence of time on the velocity profile:** In a numerical simulation process, the computation time plays an important role in the search for convergence of results. On figure 1.1 below we traced the profile of the axial velocities for a constant Reynolds number is equal to 90, with an irregular mesh  $71 * 15$ , by fixing the number of field  $Ne = 0$  and the time step at  $\Delta t = 5.10^{-2}$ . Thus the maximum number of time iterations varies from 50 to 1000, that is to say for a calculation time between 15 minutes and 4 hours. We find that the flow regime varies according to the iteration time. For relatively low times ( $t_{max} = 50$  and  $t_{max} = 100$ ) we notice that the velocity profile is parabolic. By increasing the number of iterations over time we notice a change in the shape of the curves with greater velocity. A steady state is noted from  $t_{max} = 800$ , in other words as long as the calculation time is, the result will remain the same.

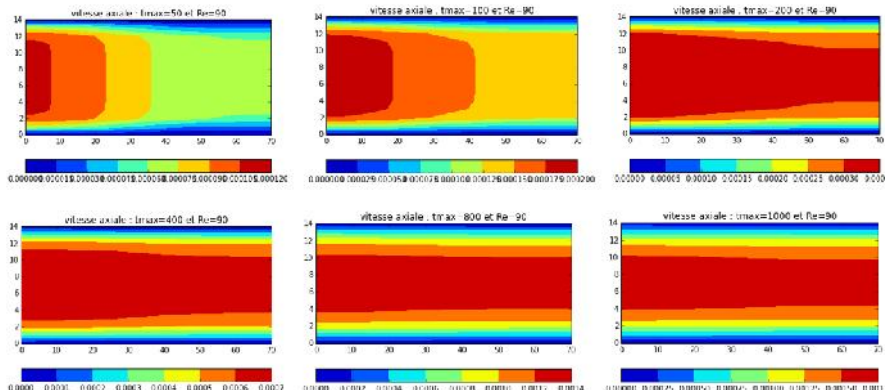


Figure 4. Influence of time on the velocity profile



**Influence of the Reynolds number on the temperature of the fluid:** The Reynolds number is the dimensionless number that characterizes the flow regime of a fluid. Its value increases with the velocity of fluid. The results of the simulations below are obtained with an iteration number fixed at 50 and a time step equal to  $\Delta t = 5.10^{-2}$ . The variations of the Reynolds number have the effect of degrading the stratification of the fluid near the walls as can be seen in the first three diagrams of Figure 5. This attenuation of the thermal boundary layer is more accentuated with the intensification of the flow for Reynolds number ranging from 425 to 600. Exceeding this number ( $Re = 600$ ) the curve lines remain the same for a flow regime laminar.

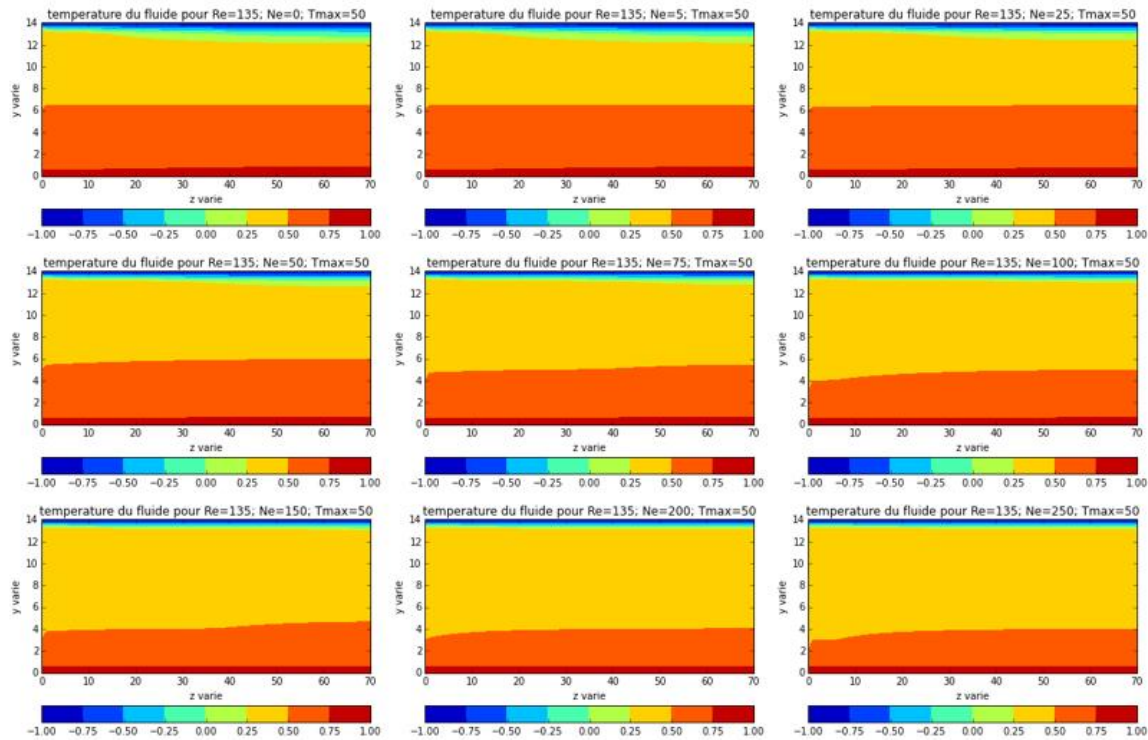


Figure 6. Influence of the number of Field Ne on the temperature of the fluid

**Variation of the Nusselt number as a function of the calculation time:** The Nusselt number is defined as being a dimensionless number which characterizes the convective transfer between a wall and a fluid. Its local and dimensionless expression can be written as a wall temperature gradient.

$$x' = \frac{x}{L}; T' = \frac{T - T_0}{T_w - T_f}; Nu = \left. \frac{\partial T'}{\partial x'} \right|_{wall}$$

We noted a difference in the results of the simulation concerning the heat transfer at the level of the upper and lower walls as a function of the duration of the simulation. In the two diagrams in Figure 7, a difference is noted on the profile of the curves. The figure on the right shows an evolution of the Nusselt number on the heated bottom wall for the same fixed Reynolds number and maximum iteration time (tmax) which varies between 50 and 1000. In the figure on the left, the same comparison is made but this time on the upper wall cooled with always the maximum time which takes values ranging from 50 to 1000.

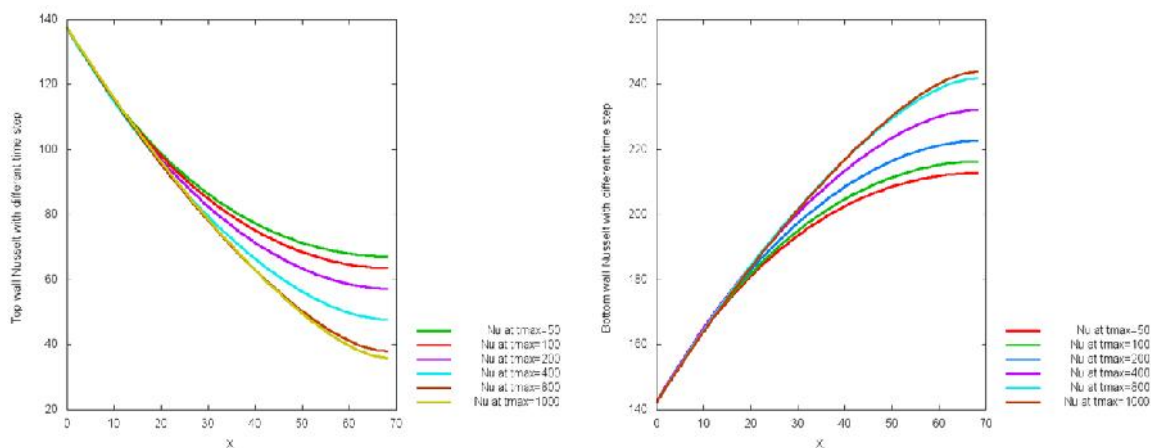


Figure 7. Variation of the Nusselt number as a function of the calculation time

Conclusion

This study allowed us to understand the phenomenon of thermomagnetic air convection in a rectangular enclosure. To properly tackle the problem, we started with an introduction accompanied by a brief bibliographic reminder of some work related to the problem raised. Mathematical and numerical modeling allowed us to pose the problem well. The mathematical equations are those of dimensionless Navier-stokes closed by initial and boundary conditions. The numerical model chooses and that of the finite volume method which is based on a discretization scheme with centered differences resolved using a FORTRAN code with the SIMPLER algorithm. Ranging from the influence of the calculation time on the velocity profile and on the variation of the Nusselt number, to the influence of the Reynolds number and the number of field (Ne) on the variation of the temperature of the fluid, we note that the results of the numerical simulation are in good agreement with those found in the literature with some differences. The results presented in this paper constitute only a part of our research work which must extend to the cases of the magneto thermal convection of a binary mixture made up of water vapor and air.

Nomenclature

A	coefficient	<u>Greek symbol</u>
B	magnetic field (T)	$\alpha$ temperature coefficient of resistance (1/C)
$C_p$	specific heat capacity (kJ/(kg. K))	$\nu$ kinematic viscosity ( $m^2/s$ )
$F_m$	magnetic force vector (N/m2)	$\rho$ density ( $kg/m^3$ )
h	tube diameter (m)	$\chi$ magnetic susceptibility per unit mass ( $m^3/kg$ )
L	length of the tube (m)	Common variables
p	static pressure (Pa)	<u>Subscripts</u>
T	temperature (K)	c cold
$T_f$	temperature of the tube walls (K)	e East face
$T_w$	averaged temperature of the tube wall (C)	f Fluid
$T_0$	inlet temperature (K)	h hot
$U_0$	reference velocity (m/s)	in inlet
u, v, w	components of velocity vector (m/s)	n north face
x, y, z	coordinates axes in computational space	s south face
		m magnetization force
		w wall
		w west face
Number without dimensions		Expressions
Nusselt ( $N_u$ )		$N_u = \frac{\partial T'}{\partial x'}$
Field number ( $N_e$ )		$N_e = \frac{\chi B_0^2}{\mu_0 U_0^2}$
Peclet number ( $P_e$ )		$P_e = \frac{2U_0}{\alpha/h}$
Reynolds number ( $R_e$ )		$R_e = \frac{2hU_0}{\nu}$

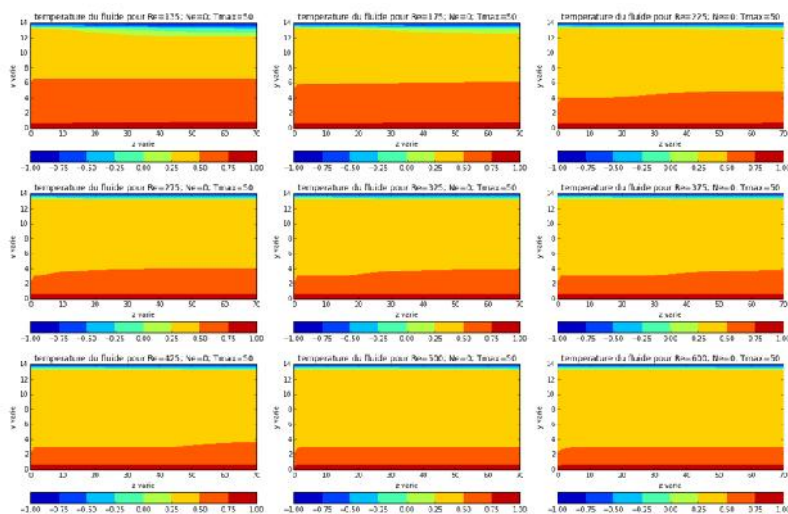


Figure 5. Influence of the Reynolds number on the temperature of the fluid

**Influence of the number of Champ (Ne) on the temperature of the fluid:** For a paramagnetic fluid flow, in certain provisions, the number of fluid (Ne) plays the same role as the Reynolds number, namely to intensify the flow regime. On the six diagrams of figure 6 we made vary the number of field (Ne) while keeping fixed the Reynolds number at 90 and the time step at  $\Delta t = 5.10^{-2}$ . By analogy to the previous case, we note that the greater the number of fields (Ne), the more the transfers between the walls and the fluid are degraded, and this for the first three diagrams of Figure 6. For field numbers between 150 and 250, there is an increased stratification due to the effect of the magnetic force, hence a weakening of the thermal limit.

## REFERENCES

ANSYS Fluent, Fluent 19.0 User's Guide

Farid Berrahil, Smail Benissad, Kamel Talbi, and Abdelouahab Bouttout. 2007. Etude d'un champ magnétique externe sur la convection naturelle dans une enceinte rectangulaire tridimensionnelle.

Masato Akamatsu, Mitsuo Higano, Yoshio Takahashi, Hiroyuki Ozoe. 2005. Numerical computation of magneto thermal convection of water in a vertical cylindrical enclosure. International Journal of Heat and Fluid Flow 26, 622-634.

Mouhamed A. Teamah, Ahmed F. Elsafty et Enass Z. Massoud. 2012. Numerical simulation of double-diffusive natural convective flow in an inclined rectangular enclosure in the presence of magnetic field and heat source. International Journal of Thermal Sciences 52, 161-175.

Patankar. SV. 2017. Transfert de chaleur numérique et écoulement de Fluides (série sur les méthodes de calcul en mécanique et sciences thermiques) (new york : Hemisphere / mcgrawhill).

Sébastien Renaudière de Vaux. (2017). Convection thermique en présence d'un champ magnétique constant, alternatif, ou d'une source de chaleur dispersée. PhD thesis.

Syou Maki. 2016. Magneto thermal Convection of Water with the Presence or Absence of a Magnetic Force Acting on the Susceptibility Gradient. PLoS ONE 11, 9.

Une procédure de calcul pour le transfert de chaleur, de masse et de quantité de mouvement dans des écoulements paraboliques tridimensionnels. In Prédiction numérique du débit, du transfert de chaleur, de la turbulence et de la combustion, pages 54-73.

Xiao-Yan Zhang, Jin-Long Zhang, Ke-Wei Song, Liang-Bi Wang. 2016. Numerical study of the sensing mechanism of the oxygen concentration sensor based on the thermal magnet convection. international journal of thermal sciences 99, 71-84.

\*\*\*\*\*